Mon. Not. R. Astron. Soc. **000**, 1–8 (2011) Printed 4 May 2012 (MN LaTeX style file v2.2)

arXiv:1111.4212v2 [astro-ph.CO] 3 May 2012

Clustering of sub-millimeter galaxies in a self-regulated baryon collapse model

Jun-Qing Xia[1]⋆, M. Negrello[2], A. Lapi[3,1], G. De Zotti[4,1], L. Danese[1], M. Viel[5,6]

[1] *Scuola Internazionale Superiore di Studi Avanzati, via Bonomea 265, I-34136 Trieste, Italy*
[2] *Dept. of Physics & Astronomy, The Open Univ., Milton Keynes MK7 6AA, UK*
[3] *Dip. Fisica, Univ. 'Tor Vergata', Via Ricerca Scientifica 1, 00133 Roma, Italy*
[4] *INAF-Osservatorio Astronomico di Padova, vicolo dell'Osservatorio 5, I-35122 Padova, Italy*
[5] *INAF-Osservatorio Astronomico di Trieste, Via G.B. Tiepolo 11, I-34131 Trieste, Italy*
[6] *INFN sez. Trieste, Via Valerio 2, 34127 Trieste, Italy*

ABSTRACT

We have investigated the Cosmic Infrared Background (CIB) anisotropies in the framework of the physical evolutionary model for proto-spheroidal galaxies by Granato et al. (2004). After having re-calibrated the cumulative flux function dS/dz at $\lambda \geqslant 850\,\mu$m using the available determinations of the shot noise amplitude (the original model already correctly reproduces it at shorter wavelengths) the CIB power spectra at wavelengths from $250\,\mu$m to 2 mm measured by *Planck*, *Herschel*, SPT and ACT experiments have been fitted using the halo model with only 2 free parameters, the minimum halo mass and the power-law index of the mean occupation function of satellite galaxies. The best-fit *minimum* halo mass is $\log(M_{\rm min}/M_{\odot}) = 12.24 \pm 0.06$, higher than, but consistent within the errors, with the estimate by Amblard et al. (2011) and close to the estimate by Planck Collaboration (2011). The redshift evolution of the volume emissivity of galaxies yielded by the model is found to be consistent with that inferred from the data. The derived *effective* halo mass, $M_{\rm eff} \simeq 5 \times 10^{12}\,M_{\odot}$, of $z \simeq 2$ sub-millimeter galaxies is close to that estimated for the most efficient star-formers at the same redshift. The effective bias factor and the comoving clustering radius at $z \simeq 2$ yielded by the model are substantially lower than those found for a model whereby the star formation is fueled by steady gas accretion, but substantially higher than those found for a merging-driven galaxy evolution with a top-heavy initial mass function.

Key words: submillimetre: galaxies – galaxies: statistics – galaxies: haloes – galaxies: high redshift.

1 INTRODUCTION

The *Herschel* surveys have allowed clustering studies (Maddox et al. 2010; Cooray et al. 2010) of sub-millimeter galaxies with a statistics at least one order of magnitude better than previously possible (Blain et al. 2004; Scott et al. 2006). These studies have been complemented by determinations of the angular power spectrum of the Cosmic Infrared Background (CIB) anisotropies on BLAST (Viero et al. 2009), *Planck* (Planck Collaboration 2011), and *Herschel* (Amblard et al. 2011) maps. Due to the unique power of sub-millimeter surveys in piercing the distant universe, thanks to the strongly negative K-correction, the clustering properties contain signatures of the large scale structure at high redshifts and can allow us to discriminate between different formation mechanisms that have been proposed for sub-millimeter galaxies. For example, merger driven galaxy evolution models, that follow the evolution of both the disk and the spheroidal components of galaxies, predict much lower clustering strengths for sub-mm galaxies (e.g. Almeida et al. 2011; Kim et al. 2011) than models whereby the star formation is fueled by steady accretion of large amounts of cold gas (e.g. Davé et al. 2010).

In this paper, building on the work by Negrello et al. (2007), we investigate the constraints set by mm and sub-mm clustering data on the physical model worked out by Granato et al. (2001, 2004) and further elaborated by Lapi et al. (2006) and Mao et al. (2007).

A specific prediction of the model is that high-z massive proto-spheroidal galaxies dominate the sub-mm counts over

---

⋆ E-mail: xia@sissa.it

a limited flux density range (cf. Lapi et al. 2011). At 250 μm the Euclidean normalized differential counts of these objects peak at $\approx$ 30 mJy; above $\simeq$ 60 mJy and below $\simeq$ 10 mJy the counts are dominated by $z \lesssim 1.5$ quiescent and starbursting late-type galaxies, less massive and less clustered than the high-z proto-spheroidal galaxies. The flux density range where proto-spheroidal galaxies dominate broadens and the peak shifts to brighter flux densities with increasing (sub-)mm wavelength. Therefore, in this scenario, the expected clustering strengths depend on the flux density range that is being probed and on wavelength.

Several other analyses of data on the angular correlation function of (sub-)mm sources and of the power spectrum of the CIB anisotropies have been carried out. They however use phenomenological parameterized models for the evolution of extragalactic sources (Hall et al. 2010; Planck Collaboration 2011; Millea et al. 2011; Pénin et al. 2011) or even of the clustering power (Addison et al. 2011). Also data at different wavelengths are usually fitted separately (Planck Collaboration 2011; Amblard et al. 2011). On the contrary, the present analysis relies on a physical model for the evolution of proto-spheroidal galaxies (although the treatment of spiral and starburst galaxies is phenomenological) and aims at accounting simultaneously for clustering data over a broad range of wavelengths, from 250 μm to a few mm.

It should be noted, however, that the physical model is exploited only to compute the cumulative flux function that weights the redshift-dependent spatial power spectrum in the Limber approximation for the angular power spectrum. The Halo Occupation Distribution (HOD), which is a statistical description of how dark matter halos are populated with galaxies, is dealt with in a simplified manner, without including the relationship between luminosity and halo mass. This is the standard practice, justified by the complexity of a thorough treatment that does not appear to be required by existing data. In the Granato et al. (2004) model the star-formation rate is related to the halo mass, *to the virialization redshift and to the age of the galaxy.* Including these additional ingredients in the analysis is impractical at the present stage. A pioneering model that explicitly includes a relationship between infrared luminosity and halo mass has been presented by Shang et al. (2011).

The plan of the paper is the following. In § 2 we present a short overview of the evolutionary model for the relevant galaxy populations. In § 3 we describe the halo model formalism used to compute the contributions to the power spectrum of Cosmic Infrared Background (CIB) anisotropies and to the angular correlation function of detected galaxies (§ 4). Our main results are presented in § 5 and our main conclusions are summarized in § 6.

We adopt a standard flat ΛCDM cosmology with $h = H_0/100\,\mathrm{km\,s^{-1}\,Mpc^{-1}} = 0.70$ and a local matter density $\Omega_{\mathrm{m}0} = 0.27$.

2 OVERVIEW OF THE MODEL

The sub-millimeter extragalactic sources are a mixed bag of various populations of dusty galaxies and of flat-spectrum radio sources (see, e.g., Lapi et al. 2011).

Our model interprets powerful high-z sub-mm galaxies as massive proto-spheroidal galaxies in the process of forming most of their stellar mass (see also Blain et al. 2004; Narayanan et al. 2010; Davé et al. 2010). It hinges upon high resolution numerical simulations showing that dark matter halos form in two stages (Zhao et al. 2003; Wang et al. 2011; Lapi & Cavaliere 2011). An early fast collapse of the halo bulk, including a few major merger events, reshuffles the gravitational potential and causes the dark matter and the stellar component to undergo (incomplete) dynamical relaxation. A slow growth of the halo outskirts in the form of many minor mergers and diffuse accretion follows; this second stage has little effect on the inner potential well where the visible galaxy resides.

The star formation is triggered by the fast collapse/merger phase of the halo and is controlled by self-regulated baryonic processes. It is driven by the rapid cooling of the gas within a region of $\simeq 70(M_h/10^{13}\,M_\odot)^{1/3}[(1+z)/3]^{-1}$ kpc, where M_h is the halo mass, is regulated by the energy feedback from supernovae (SNe) and Active Galactic Nuclei (AGNs), is very soon obscured by dust and is stopped by quasar feedback. The AGN feedback is relevant especially in the most massive galaxies and is responsible for their shorter duration ($5-7\times10^8$ yr) of the active star-forming phase. In less massive proto-spheroidal galaxies the star formation rate is mostly regulated by SN feedback and continues for a few Gyr.

Since spheroidal galaxies are observed to be in passive evolution at $z \lesssim 1-1.5$ (e.g., Renzini 2006), they are visible at sub-mm wavelength only at high redshifts. Lapi et al. (2011) have shown that the Granato et al. (2004) model, as further elaborated by Lapi et al. (2006), provides a reasonably good fit to the observed counts from 250 μm to $\simeq$ 1 mm as well as to the luminosity functions in the range $z = 1-4$ and to the redshift distributions at $z > 1$ estimated from *Herschel*-ATLAS (Eales et al. 2010) data.

The fit was obtained using of a single SED (that of the well studied $z = 2.3$ strongly lensed galaxy SMM J2135-0102, "The Cosmic Eyelash"; Ivison et al. 2010, Swinbank et al. 2010) for the whole population of proto-spheroidal galaxies. This is obviously an oversimplification and indeed the Lapi et al. (2011) counts are somewhat high at mm wavelengths, especially at relatively bright flux densities. As a consequence, the model overestimates the Poisson (shot-noise) contribution to the power spectrum of intensity fluctuations since such contribution is directly related to the source counts [see eq. (21)]. Consistency with the shot-noise levels estimated by Planck Collaboration (2011) at 353 GHz and measured by Hall et al. (2010), Dunkley et al. (2011) at 220 and 150 GHz is recovered scaling down the cumulative flux function dS/dz [see eq. (19)] of proto-spheroidal galaxies by a factor of 0.81, 0.71, and 0.55 at 353, 217, and 150 GHz (850 μm, 1.38 mm, 2 mm), respectively. No correction was applied at higher frequencies. In practice, we use the determination of the shot noise amplitude to recalibrate the function dS/dz to be used to compute the clustering power spectrum, which is measured independently. This correction mimics the effect of adopting a SED decreasing with increasing wavelength beyond the peak a bit more steeply than the one adopted by Lapi et al. (2011).

As suggested in the latter paper, the overestimate of mm-wave counts may be cured if higher-z galaxies, that yield larger and larger contributions to the bright counts at increasing mm wavelengths, have SEDs slightly hotter than

SMM J2135-0102 and closer to that of G15.141 (Cox et al. 2011; see Fig. 2 of Lapi et al. 2011). We have checked that indeed a good fit of the counts at all the frequencies considered here is obtained using the SMM J2135-0102 SED for galaxies at $z < 3.5$ and the SED of G15.141 at higher z. However the match of the frequency spectrum of the shot-noise amplitude also improves but not enough to reach consistency with observational estimates at the longer wavelengths. Since the shot noise amplitude can be computed directly from the counts, this suggests that there may be some small, but non-negligible, offsets between the calibration of point source flux densities and that of the diffuse background. This is not surprising since, in addition to the possibility of an imperfect photometric calibration, at mm wavelengths the recovery of the contribution of dusty galaxies to the power spectrum requires a delicate subtraction of the other components (Cosmic Microwave Background, cirrus emission, fluctuations due to radio sources). A rescaling to match the shot noise spectrum seems to be the only practical way for correcting for these offsets. Since the modification is only significant at $\geqslant 850\,\mu$m (in the observer frame), i.e. well beyond the peak for most sources, the impact on the bolometric luminosity, which is related to the halo mass, is minor. For galaxies at redshifts up to $z = 3.5$, accounting for essentially all the signal, the bolometric luminosity varies by $\leqslant 2\%$. For comparison, the coefficient of the relationship between the star formation rate (SFR; given by the model) and the bolometric luminosity has an uncertainty of $\sim 30\%$ (Kennicutt 1998).

The Granato et al. (2004) model is meant to take into account the star formation occurring within galactic dark-matter halos virialized at $z_{\rm vir} \gtrsim 1.5$ and bigger than $M_{\rm vir} \simeq 10^{11.2} M_\odot$, which are, crudely, associated to massive spheroidal galaxies. We envisage disk (and irregular) galaxies as associated primarily to halos virializing at $z_{\rm vir} \lesssim 1.5$, which have incorporated, through merging processes, a large fraction of halos less massive than $10^{11.2}\,M_\odot$ virializing at earlier times, which may become the bulges of late type galaxies. The model, however, does not follow the formation and evolution of disk and bulge components of galaxies. For spiral and starburst galaxies we adopt the phenomenological model described by Negrello et al. (2007). On the other hand, as shown in the following, these galaxies are essentially non influential for the purposes of the present paper in the considered frequency range: proto-spheroids dominate the contributions both to the power spectrum of fluctuations and to the angular correlation function of detected sources.

Because of the strong dilution due to their very broad luminosity function, the contribution of radio sources to the clustering power spectrum can be safely neglected in the wavelength range considered here. Their contribution to Poisson fluctuations was computed using the De Zotti et al. (2005) model.

3 HALO MODEL FORMALISM

To compare the clustering properties expected from our model with observational data we adopt the halo model formalism (Cooray & Sheth 2002). The power spectrum of the galaxy distribution is parameterized as the sum of the 1-halo term, that dominates on small scales and depends on the distribution of galaxies within the same halo, and the 2-halo term, that dominates on large scales and is related to correlations among different halos:

$$P_{\rm gal}(k,z) = P^{\rm 1h}_{\rm gal}(k,z) + P^{\rm 2h}_{\rm gal}(k,z), \tag{1}$$

$$P^{\rm 1h}_{\rm gal}(k,z) = \int_M dM \frac{dn}{dM} \frac{\langle N_{\rm gal}(N_{\rm gal}-1)\rangle}{\bar{n}^2_{\rm gal}} |u_{\rm gal}(k,M)|^s, \tag{2}$$

$$P^{\rm 2h}_{\rm gal}(k,z) = P_{\rm lin}(k,z)\left[\int_M dM \frac{dn}{dM} \frac{\langle N_{\rm gal}\rangle}{\bar{n}_{\rm gal}} b(M,z) u_{\rm gal}(k,M)\right]^2, \tag{3}$$

where dn/dM is the halo mass function (Sheth & Tormen 1999) and the linear matter power spectrum, $P_{\rm lin}(k,z)$, has been computed using the CAMB code[1] (Lewis, Challinor & Lasenby 2000). Here, $u_{\rm gal}(k,M)$ denotes the Fourier transform of the mass density profile of the galaxy distribution within the dark matter halo, that we assume to be approximately the same as that of the dark matter, i.e. we take $u_{\rm gal}(k,M) \simeq u_{\rm dm}(k,M)$.

$\langle N_{\rm gal}\rangle$ is the mean number of galaxies in a halo of mass M, subdivided in "central" and "satellite" galaxies ($\langle N_{\rm gal}\rangle = \langle N_{\rm cen}\rangle + \langle N_{\rm sat}\rangle$), while $\bar{n}_{\rm gal}$ is the mean number density of galaxies:

$$\bar{n}_{\rm gal} = \int_M dM \frac{dn}{dM} \langle N_{\rm gal}\rangle. \tag{4}$$

We model the HOD using a central-satellite formalism (see, e.g., Zheng et al. 2005): this assumes that the first galaxy to be hosted by a halo lies at its center, while any remaining galaxies are classified as satellites and are distributed in proportion to the halo mass profile. Following Tinker & Wetzel (2010), the mean occupation functions of central and satellite galaxies are parameterized as:

$$\langle N_{\rm cen}\rangle = \frac{1}{2}\left[1 + {\rm erf}\left(\frac{\log_{10}(M/M_{\rm min})}{\sigma(\log_{10} M)}\right)\right], \tag{5}$$

$$\langle N_{\rm sat}\rangle = \frac{1}{2}\left[1 + {\rm erf}\left(\frac{\log_{10}(M/2M_{\rm min})}{\sigma(\log_{10} M)}\right)\right]\left(\frac{M}{M_{\rm sat}}\right)^{\alpha_{\rm sat}}, \tag{6}$$

where $M_{\rm min}$, $\alpha_{\rm sat}$, $M_{\rm sat}$, and $\sigma(\log_{10} M)$ are free parameters assumed to be redshift independent. In this formalism halos below $M_{\rm min}$ do not contain galaxies while halos above this threshold contain a central galaxy plus a number of satellite galaxies with a power-law mass function with slope $\alpha_{\rm sat}$.

The mean mass density profile of halos of mass M is (Navarro, Frenk, & White 1996):

$$\rho(r) = \frac{\rho_{\rm s}}{(r/r_{\rm s})(1+r/r_{\rm s})^2}, \tag{7}$$

$$M = 4\pi\rho_{\rm s} r_{\rm s}^3\left[\log(1+c) - \frac{c}{1+c}\right], \tag{8}$$

with $c = r_{\rm vir}/r_{\rm s}$. The normalized Fourier transform of this profile is:

$$u_{\rm dm}(k,M) = \frac{4\pi\rho_{\rm s} r_{\rm s}^3}{M}\left\{\sin(kr_{\rm s})\left[Si([1+c]kr_{\rm s}) - Si(kr_{\rm s})\right] + \cos(kr_{\rm s})\left[Ci([1+c]kr_{\rm s}) - Ci(kr_{\rm s})\right] - \frac{\sin(ckr_{\rm s})}{(1+c)kr_{\rm s}}\right\}, \tag{9}$$

---

[1] http://camb.info/

where Si and Ci are the sine and cosine integrals, respectively:

$$Si(x) = \int_0^x \frac{\sin(t)}{t}dt, \quad Ci(x) = -\int_x^\infty \frac{\cos(t)}{t}dt. \qquad (10)$$

Following Bullock et al. (2001), we approximate the dependence of the concentration c on M and z as

$$c(M,z) = \frac{9}{1+z}\left(\frac{M}{M_*}\right)^{-0.13} \qquad (11)$$

where $M_*(z)$ is the characteristic mass scale at which $\nu(M,z) = 1$; $M_*(z=0) \simeq 5\times 10^{12}\,h^{-1}\,M_\odot$.

In the 1-halo term [eq. (2)] we set $s = 2$, in analogy with the corresponding term for the dark matter power spectrum, if $\langle N_{\rm gal}(N_{\rm gal}-1)\rangle > 1$. Otherwise we set $s = 1$ since if the halo contains only one galaxy, it will sit at the center. Taking into account that $\langle N_{\rm gal}(N_{\rm gal}-1)\rangle \simeq 2\langle N_{\rm cen}\rangle\langle N_{\rm sat}\rangle + \langle N_{\rm sat}\rangle^2$ and that only the galaxies that are not at the center get factors of $u_{\rm gal}(k,M) \simeq u_{\rm dm}(k,M)$ we have:

$$P^{\rm 1h}_{\rm gal}(k,z) = \frac{1}{\bar{n}^2_{\rm gal}}\int_M dM\frac{dn}{dM}\cdot$$
$$\cdot\quad \left[2\langle N_{\rm cen}\rangle\langle N_{\rm sat}\rangle u_{\rm dm}(k,M) + \langle N_{\rm sat}\rangle^2 u^2_{\rm dm}(k,M)\right], \qquad (12)$$

$$P^{\rm 2h}_{\rm gal}(k,z) = P_{\rm lin}(k,z)\cdot$$
$$\cdot\quad \left[\int_M dM\frac{dn}{dM}\frac{\langle N_{\rm gal}\rangle}{\bar{n}_{\rm gal}}b(M,z)u_{\rm dm}(k,M)\right]^2, \qquad (13)$$

with $(dn/dM)dM = f(\nu)(\rho_{\rm m}/M)d\nu$,

$$\bar{n}_{\rm gal} = \int_M dM\frac{dn}{dM}\langle N_{\rm gal}\rangle = \int_\nu d\nu f(\nu)\left(\frac{\rho_{\rm m}}{M}\right)\langle N_{\rm gal}\rangle, \qquad (14)$$

and $\rho_{\rm m}/M = 3/(4\pi R^3)$. On large scales, where the 2-halo term dominates, $u_{\rm dm}(k,M) \to 1$ and $P^{\rm 2h}_{\rm dm}(k,z) \simeq b^2_{\rm gal}P_{\rm lin}(k,z)$ with:

$$b_{\rm gal}(z) = \int_\nu d\nu f(\nu)\left(\frac{\rho_{\rm m}}{M}\right)b(M,z)\frac{\langle N_{\rm gal}\rangle}{\bar{n}_{\rm gal}}. \qquad (15)$$

We also define the effective large-scale bias, $b_{\rm eff}(z)$, as

$$b_{\rm eff}(z) = \int_M dM\,\frac{dn}{dM}\,\frac{\langle N_{\rm gal}\rangle}{\bar{n}_{\rm gal}}b(M,z), \qquad (16)$$

and the effective mass of the halo, $M_{\rm eff}$,

$$M_{\rm eff}(z) = \int_M dM\,\frac{dn}{dM}M\frac{\langle N_{\rm gal}\rangle}{\bar{n}_{\rm gal}}. \qquad (17)$$

4 ANGULAR POWER SPECTRUM OF INTENSITY FLUCTUATIONS

The angular power spectrum $P(k_\theta)$ of intensity fluctuations due to clustering of sources fainter than some flux density limit $S_{\rm lim}$ is a projection of the spatial power spectrum of such sources at different redshifts z, $P_{\rm gal}(k,z)$. In the Limber approximation, valid if the angular scale is not too large (i.e. $2\pi k_\theta \geqslant 10$), the relation between $P_{\rm gal}(k,z)$ and $P(k_\theta)$ is:

$$P(k_\theta) = \int_{z_{\rm min}}^{z_{\rm max}} dz\,P_{\rm gal}\left(k = \frac{2\pi k_\theta + 1/2}{\chi(z)}, z\right)\left(\frac{dS}{dz}(z)\right)^2\frac{dz}{dV_{\rm c}}, \quad (18)$$

where dS/dz is the redshift distribution of the cumulative flux of sources with $S \leqslant S_{\rm lim}$

$$\frac{dS}{dz} = \int_0^{S_{\rm lim}} d\log_{10}(S)\,S\,\phi[L(S,z),z]\,\frac{dV_{\rm c}}{dz}, \qquad (19)$$

$\phi(L,z)$ is the epoch-dependent comoving luminosity function per unit interval of $\log_{10}(L)$, and $dV_{\rm c}$ is the comoving volume element, $dV_{\rm c} = \chi^2 d\chi$, $\chi(z)$ being the comoving radial distance:

$$\chi(z) = \frac{c}{H_0}\int_0^z \frac{dz'}{\sqrt{\Omega_{\rm m0}(1+z')^3 + (1-\Omega_{\rm m0})}}. \qquad (20)$$

Poisson fluctuations add a white noise contribution to the power spectrum of fluctuations:

$$P_{\rm shot} = \int_0^{S_{\rm lim}} \frac{dN}{d\log_{10} S}\,S^2\,d\log_{10} S, \qquad (21)$$

with

$$\frac{dN}{d\log_{10} S} = \int dz\,\phi[L(S,z),z]\,\frac{dV_{\rm c}}{dz}. \qquad (22)$$

We have computed the functions dS/dz for each galaxy population using the the cosmological model specified in § 1 and the evolutionary models briefly described in § 2. As mentioned in § 2, the functions dS/dz for proto-spheroidal galaxies at frequencies $\leqslant 353\,$GHz ($\lambda \geqslant 850\,\mu$m) have been scaled down by constant factors to comply with the measurements or the best estimates of the shot-noise levels. At higher frequencies our model accurately fits the observed source counts and therefore provides directly reliable estimates of the shot noise level.

We have chosen to deal with the shot noise and the clustering contributions to the power spectrum of CIB fluctuations independently of each other because the former are independent of the parameters describing the clustering and are strongly constrained by the available source counts. Moreover, when only relatively low resolution data are available, as is the case for *Planck*, there is a degeneracy between the shot-noise and the 1-halo clustering term. As clearly highlighted by Planck Collaboration (2011), an unsupervised least-square fit of the full CIB power spectrum measured by *Planck*, taking the shot-noise amplitude as a free parameter, leads to fits of similar quality with and without a substantial contribution from the 1-halo term. But fits with a low contribution from the 1-halo term imply shot noise amplitudes far in excess of those estimated from the source counts. The higher resolution of *Herschel*, SPT and ACT data breaks the degeneracy at $\nu \geqslant 600\,$GHz and at $\nu \leqslant 220\,$GHz, respectively, allowing a direct estimate of the shot-noise amplitude.

As for the halo model, we have considered two distinct populations, i.e. proto-spheroidal galaxies and late-type galaxies, both quiescent and starbursting. Taking into account the constraints on clustering of late-type galaxies coming from IRAS data (Mann et al. 1995; Hawkins et al. 2001) we find that the contribution of these sources is always sub-dominant and, correspondingly, their halo model parameters are very poorly constrained. Moreover the values of $M_{\rm sat}$ and $\sigma(\log_{10} M)$ are poorly constrained also for proto-spheroidal galaxies (Planck Collaboration 2011). We have therefore fixed $M_{\rm sat} = 20M_{\rm min}$ and $\sigma(\log_{10} M) = 0.6$ [within the ranges found by Tinker & Wetzel (2010) from clustering studies of optical galaxies] for both populations, and $M_{\rm min,late-type} = 10^{11}\,M_\odot$ and $\alpha_{\rm sat,late-type} = 1$. We are

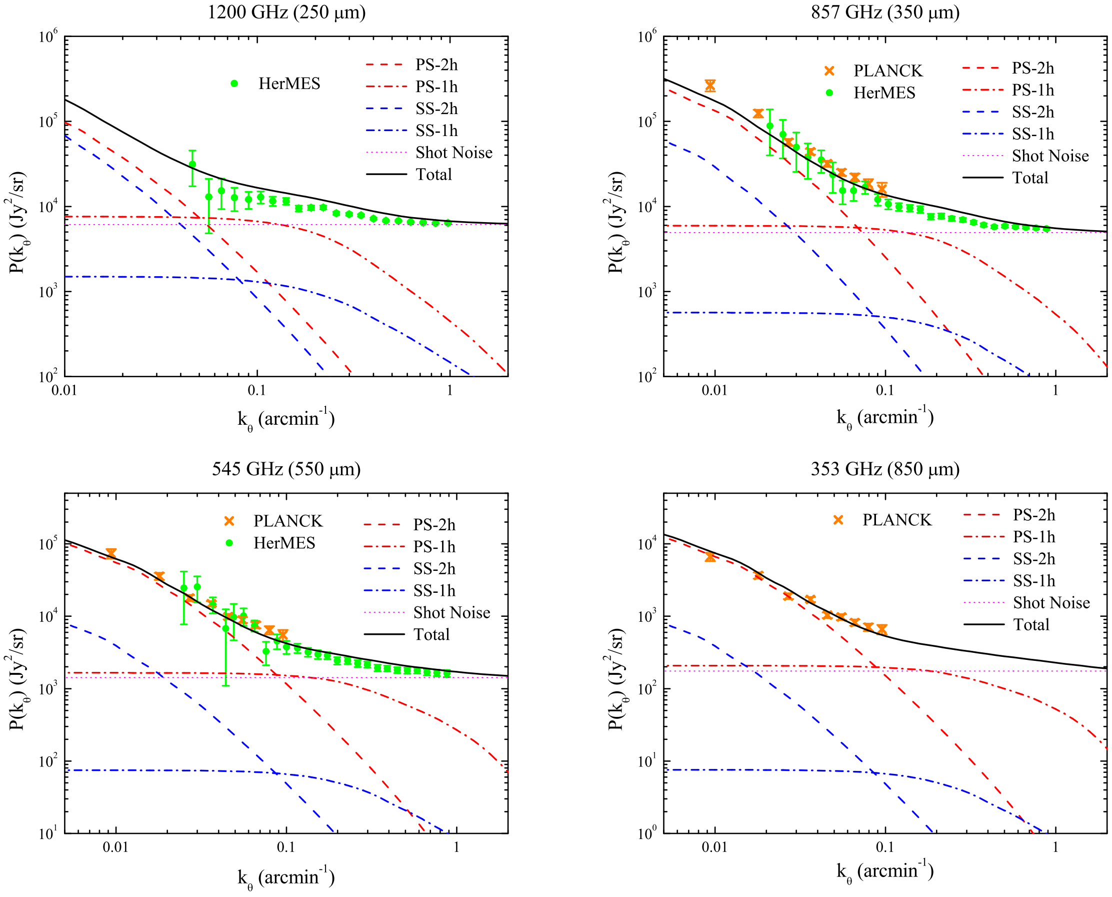

Figure 1. CIB angular power spectra $P(k_\theta)$ at sub-mm wavelengths. Data from Planck Collaboration (2011) and *Herschel*/HerMES (Amblard et al. 2011). For the *Herschel*/HerMES data at 350 and 500 μm we have adopted the values corrected by Planck Collaboration (2011). At 250 μm we have used the values given by Amblard et al. (2011), that may be underestimated because of an over-subtraction of the cirrus contamination and a slight overestimate of the effective beam area. The conversion from the multipole number ℓ used by Planck Collaboration (2011) and the wavenumber $k\,(\mathrm{arcmin}^{-1})$ is $k = \ell/(2 \times 180 \times 60)$. The lines show the contributions of the 1-halo and 2-halo terms for the two populations considered here [spiral and starburst (SS), and proto-spheroidal (PS) galaxies]. The magenta horizonal lines denote the shot noise level.

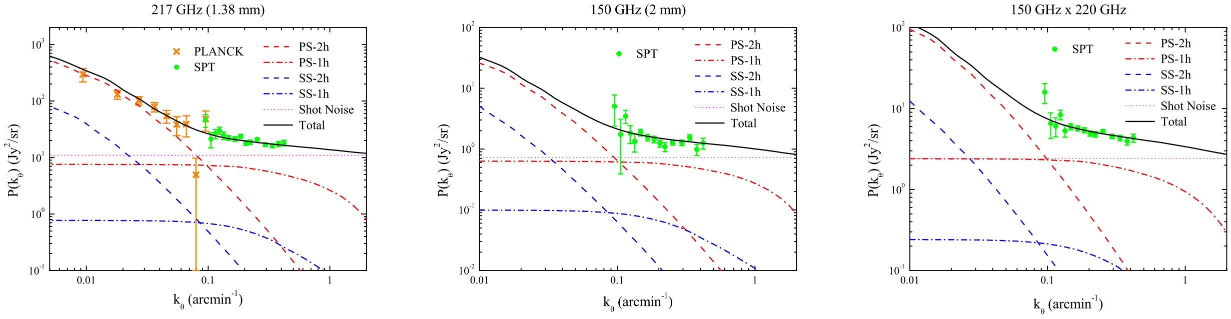

Figure 2. CIB angular power spectra $P(k_\theta)$ at mm wavelengths and 150×220 GHz cross spectrum. Data from Planck Collaboration (2011) and SPT (Hall et al. 2010; Shirokoff et al. 2011). The ACT data (Dunkley et al. 2011; Das et al. 2011) are in good agreement with the SPT ones and are not plotted to avoid over-crowding the figure. The lines have the same meaning as in Fig. 1.

then left with only 2 free parameters, i.e. $M_{\rm min}$ and $\alpha_{\rm sat}$, for proto-spheroidal galaxies.

The angular power spectra of CIB anisotropies at 217, 353, 545, and 857 GHz on the multipole range $200 \leqslant \ell \leqslant 2000$ have been determined by Planck Collaboration (2011) using *Planck* maps of six regions of low Galactic dust emission with a total area of $140\,\deg^2$. In the same paper, the power spectrum measurements by Amblard et al. (2011), using *Herschel*/SPIRE data at 250, 350, and 500 μm and extending down to sub-arcmin angular scales, i.e. up to $\ell \sim 2 \times 10^4$, were re-analyzed. It was found that Amblard et al. (2011) overestimated the correction for contamination by Galactic cirrus. Moreover, the diffuse-emission calibration of SPIRE data was improved using the more accurate *Planck*/HFI calibration. We have used the Amblard et al. (2011) data as corrected by Planck Collaboration (2011) at 350 and 500 μm. No correction could be applied at 250 μm so that the data points at this wavelength could be underestimated.

Power spectrum measurements at mm wavelengths (around 150 and 220 GHz) have been obtained with the SPT and the ACT (Hall et al. 2010; Dunkley et al. 2011; Shirokoff et al. 2011; Das et al. 2011). The subtraction of the other components (CMB, Sunyaev-Zeldovich effect, radio sources) has been done using the best fit values given in the papers. Note that the units quoted as μK^2 are actually μK$^2\times$sr. The conversion factor from these units to Jy^2/sr is $\simeq [24.8(x^2/\sinh(x/2))]^2/[2\ell(\ell+1)]$. The factor $[24.8(x^2/\sinh(x/2))]^2$ is $\simeq 1.55 \times 10^5$ at 150 GHz and $\simeq 2.34 \times 10^5$ at 217 GHz.

The angular correlation function $w(\theta)$ for a single source population writes, in terms of the 2D power spectrum $P(k_\theta)$:

$$w(\theta) = 2\pi \int_0^\infty k_\theta P(k_\theta) J_0(2\pi k_\theta \theta) dk_\theta, \tag{23}$$

where J_0 is the Bessel function of order 0.

Here we have two sub-populations, proto-spheroidal and spirals+starburst galaxies, with different clustering properties. If their cross-correlations can be ignored the signal for the whole is given by (Wilman et al. 2003):

$$w_{\rm tot}(\theta) = f_{\rm PS}^2 w_{\rm PS}(\theta) + f_{\rm SS}^2 w_{\rm SS}(\theta), \tag{24}$$

where $f_{\rm PS}$ and $f_{\rm SS}$ are the fractional contributions of proto-spheroidal and spirals+starburst galaxies, respectively, to the total counts:

$$f_{\rm PS/SS} = \frac{\int dz \mathcal{N}_{\rm PS/SS}(z)}{\int dz \mathcal{N}_{\rm tot}(z)}\ , \tag{25}$$

$\mathcal{N}$ being the redshift distribution. Ignoring the cross-correlations between the two source populations is justified because of the widely different redshift distributions implied by the adopted evolutionary model: as mentioned in § 2, proto-spheroidal galaxies are associated to galactic-size halos virialized at $z_{\rm vir} \gtrsim 1.5$ while disk (and irregular/starburst) galaxies are associated primarily to halos virializing at $z_{\rm vir} \lesssim 1.5$.

The spatial correlation function $\xi(r, z)$ is the Fourier anti-transform of the 3D power spectrum:

$$\xi(r, z) = \frac{1}{2\pi^2} \int_0^\infty k^2\, P_{\rm gal}(k) \left(\frac{\sin(kr)}{kr}\right) dk. \tag{26}$$

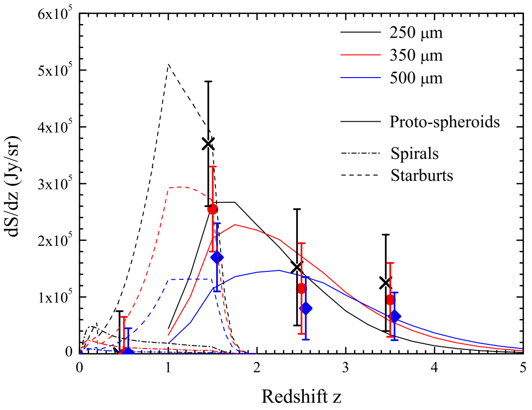

Figure 3. Redshift evolution of the galaxy intensities at 250, 350, and 500 μm yielded by the model compared with the observation-based estimates by Amblard et al. (2011). The different line styles correspond to the different sub-populations, as specified in the inset. Some caution is needed in interpreting these data, in view of the problems pointed out by Planck Collaboration (2011; see text).

The clustering radius $r_0(z)$ is defined by $\xi(r_0, z) = 1$.

5 RESULTS

Figures 1 and 2 compare the best fit model power spectrum with *Planck*, *Herschel*, and SPT data in the wavelength range 250 μm$-$2 mm. The agreement is generally good except at 250 μm where the model is consistently above the data points by Amblard et al. (2011) which, however, could be underestimated (see § 4). As mentioned above, we have only two free parameters, i.e. the minimum mass and the power-law index of the mean occupation function of satellite galaxies of proto-spheroidal galaxies. The constraints we obtain are $\log(M_{\rm min}/M_\odot) = 12.24 \pm 0.06$ and $\alpha_{\rm sat} = 1.81 \pm 0.04$ ($1\,\sigma$). The nominal errors on each parameter have been computed marginalizing on the other and correspond to $\Delta\chi^2 = 1$. We caution that the true uncertainties are likely substantially higher than the nominal values, both because the model relies on simplifying assumptions that may make it too rigid and because of possible systematics affecting the data.

The fact that the same values of these parameters account for the clustering data from 2 mm to 250 μm confirms the conclusion by Planck Collaboration (2011) that CIB fluctuations over this wavelength range are dominated by a single sub-population of dusty galaxies. According to our model, this sub-population is made of proto-spheroidal galaxies making most of their stars at $z > 1$. We find that only at 250 μm other dusty galaxy populations, normal disk and starburst galaxies, make a significant, but still sub-dominant contribution to the clustering power spectrum. As shown by Lapi et al. (2011), according to our model, proto-spheroidal galaxies also account for the bulk of the CIB intensity in this wavelength range, consistent with the finding by Planck Collaboration (2011) that the CIB anisotropies have the same frequency spectrum as the CIB intensity.

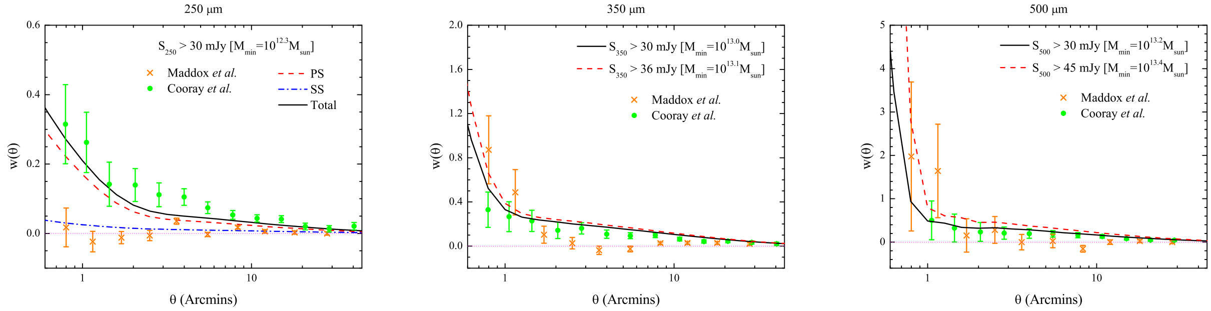

Figure 4. Angular correlation function of sub-mm galaxies. Data from Cooray et al. (2010) and Maddox et al. (2010). In the left-hand panel the dashed and dash-dotted lines show the contributions of PS and SS populations, while the solid line denotes the total angular correlation function. In other two panels, the dashed and solid lines show the global model correlation functions for the limiting flux densities adopted in the analyses by Maddox et al. and Cooray et al., respectively. The horizontal dotted line shows the zero level.

Our estimate of the minimum mass is higher than, but consistent, within the errors, with those found by Amblard et al. (2011) considering a single galaxy population and 5 free parameters per frequency (but one of the parameters is unconstrained by the data within the prior range): $\log(M_{\rm min}/M_\odot) = 11.1^{+1.0}_{-0.6}$ at $250\,\mu$m, $\log(M_{\rm min}/M_\odot) = 11.5^{+0.7}_{-0.2}$ at $350\,\mu$m, and $\log(M_{\rm min}/M_\odot) = 11.8^{+0.4}_{-0.3}$ at $500\,\mu$m. Our value of $\alpha_{\rm sat}$ is also consistent with those by Amblard et al.: $\alpha_{\rm sat} = 1.6^{+0.1}_{-0.2}$ at $250\,\mu$m, $\alpha_{\rm sat} = 1.8^{+0.1}_{-0.7}$ at $350\,\mu$m and $500\,\mu$m. In Planck Collaboration (2011) two or three free parameters *per frequency* were used; the derived minimum masses are in the range $\log(M_{\rm min}/M_\odot) = 11.8 - 12.5$.

There is however an interesting difference with Planck Collaboration (2011), due to the different redshift distributions of sources. The crossover between the 1-halo and the 2-halo term occurs, according to the model by Planck Collaboration (2011), at multipole numbers ranging from $\ell \simeq 800$ at 857 GHz ($350\,\mu$m) to $\ell \simeq 1200$ at 217 GHz (1.38 mm) corresponding to angular scales ranging from $\theta \simeq 180\times 60/\ell \simeq 13.5'$ at 857 GHz to $9'$ at 217 GHz. According to the Béthermin et al. (2011) model used in that paper, the contribution to the CIB intensity at 857 GHz peaks at $z \simeq 1$ where the angular scale of $13.5'$ corresponds to a physical linear scale $L \simeq 6.5$ Mpc; at 217 GHz the bulk of the CIB contribution comes from $z > 2$ where an angular scale of $9'$ corresponds to a physical linear scale $L \simeq 4.5$ Mpc. The non-linear masses corresponding to an overdensity $\Delta_c = 1.68$ on these scales are $M_{\rm nl}(z = 1; L = 6.5{\rm Mpc}) \simeq 7 \times 10^{13}\,M_\odot$ and $M_{\rm nl}(z = 2; L = 4.5{\rm Mpc}) \simeq 8 \times 10^{13}\,M_\odot$, respectively. For comparison, the characteristic non-linear masses computed from $\sigma(M_*, z) = 1.68$ ($\sigma(M_*, z)$ being the rms overdensity) are $M_*(z = 1) = 2\times10^{11}\,M_\odot$ and $M_*(z = 2) = 7.3\times10^{9}\,M_\odot$. This suggests that structures going non-linear on the considered scales are extremely rare at the corresponding redshifts. This potential difficulty is eased in our model because the crossover scales are lower by almost a factor of 2. As shown by Figs. 1 and 2, the 1-halo/2-halo crossover occurs at $\ell \simeq 1450$ at 857 GHz and at $\ell \simeq 2100$ at 217 GHz, corresponding to angular scales of $7.4'$ and $5.1'$, respectively.

Our value of $M_{\rm min}$ implies an effective halo mass [eq. (17)] at $z \simeq 2$ of proto-spheroidal galaxies, making up most of the CIB, $M_{\rm eff} \simeq 5 \times 10^{12}\,M_\odot$, close to the estimated halo mass of the most effective star formers in the universe. Tacconi et al. (2008) estimated their mean comoving density at $z \sim 2$ to be $\sim 2 \times 10^{-4}\,{\rm Mpc}^{-3}$. For the standard ΛCDM cosmology this implies that they are hosted by dark matter halos of $\sim 3.5 \times 10^{12}\,M_\odot$ (Dekel et al. 2009).

Figure 3 compares the flux density coming from different redshifts, dS/dz [eq. (19)], predicted by the model at the SPIRE wavelengths with the best fit estimates by Amblard et al. (2011). Planck Collaboration (2011) give (their Table 7) the best fit values of the redshift-independent volume emissivity, $j_{\rm eff}$, for $z > 3.5$ [their eq. (43)]. The values of $j_{\rm eff}$ given by our model (52, 175, 265, and 205 $\rm Jy\,sr^{-1}\,Mpc^{-1}$ at 217, 353, 545, and 857 GHz, respectively) are consistent with the best-fit results.

As for the angular correlation function, $w(\theta)$, of detected SPIRE galaxies, Cooray et al. (2010) reported measurements of $w(\theta)$ for sources brighter than 30 mJy at all SPIRE wavelengths and inferred values of $\log(M_{\rm min}/M_\odot)$ ranging from $12.6^{+0.3}_{-0.6}$ at $250\,\mu$m to $13.5^{+0.3}_{-1.0}$ at $500\,\mu$m. On the other hand, Maddox et al. (2010) did not detect a significant clustering for their $250\,\mu$m selected sample with a flux limit of $33\,{\rm mJy\,beam}^{-1}$, but detected strong clustering at $350\,\mu$m and $500\,\mu$m, albeit with relatively large uncertainties. Our model entails a relationship between the far-IR/sub-mm luminosity of proto-spheroidal galaxies (that provide the dominant contribution to $w(\theta)$, see the left-hand panel of Fig. 4) and the associated halo masses (Lapi et al. 2011). For the flux density limit adopted by Cooray et al. (2010), 30 mJy at all SPIRE wavelengths, the model yields $\log(M_{\rm min}/M_\odot) \simeq 12.3$, 13, and 13.2 at 250, 350, and $500\,\mu$m, respectively, while for the flux density limits of Maddox et al. (2010; 33, 36, and 45 mJy) we have $\log(M_{\rm min}/M_\odot) \simeq 12.3$, 13.1, and 13.4. The corresponding predictions for $w(\theta)$ are compared with the data in Fig. 4. The agreement of the model with the data is generally good, although the situation at $250\,\mu$m is unclear since there is a discrepancy between the Cooray et al. (2010) and the Maddox et al. (2010) results.

6 DISCUSSION AND CONCLUSIONS

According to the Granato et al. (2004) model, the steep portion of sub-mm counts is dominated by massive proto-spheroidal galaxies in the process of forming most of their stars on a timescale varying with halo mass (shorter for more massive galaxies), but typically of $\simeq 0.7$ Gyr, i.e. with a duty cycle of $\simeq 0.2$ at $z \simeq 2$, where their redshift distribution peaks. As shown above, this model allows us to reproduce the power spectrum of CIB fluctuations over a broad frequency range, from $250\,\mu$m to a few mm, with only 2 free parameters. The model also yields an effective volume emissivity at different redshifts consistent with observational estimates. The derived effective halo mass, $M_{\rm eff} \simeq 5\times10^{12}\,M_\odot$, is close to that estimated for the most efficient star-formers at $z \simeq 2$.

The multipole number at which the 1-halo term starts exceeding the 2-halo contribution to the clustering power spectrum ranges from $\ell = 1450$ at 857 GHz to $\ell = 2100$ at 217 GHz. These values are almost a factor of 2 higher (and, consequently, the corresponding angular scales are almost a factor of 2 lower) than those found by Planck Collaboration (2011). Since, at the redshifts where the contribution to the CIB intensity peaks, the corresponding masses are well above M_*, this difference translates into a much larger abundance of the relevant halos.

Alternative models make quite different predictions for the clustering properties of sub-mm galaxies. A widespread view is that these objects are powered by major merger events. Two major theories have been worked out in this general framework. One view is that sub-mm galaxies are massive objects, seen during a short-duration, intense, merger-induced burst of star formation (e.g. Narayanan et al. 2009). Since massive galaxies are rare at high-z and, because of the short duration of the burst, only a small fraction of them are in the sub-mm bright phase at a given time, this scenario has difficulty in reproducing the observed counts. This difficulty may be overcome assuming an extremely top-heavy initial stellar mass function that would allow much less massive (hence far more abundant) galaxies to reach the required luminosities (e.g. Baugh et al. 2005; Lacey et al. 2010).

The clustering implied by the latter scenario has been investigated by Almeida et al. (2011) who found, at $z = 2$, a comoving correlation length of $r_0 = 5.6 \pm 0.9\,h^{-1}$ Mpc for galaxies with $850\,\mu$m flux densities brighter than 5 mJy or an effective bias factor $b_{\rm eff} = 2.3$; for galaxies with $S_{450\mu{\rm m}} > 5$ mJy they found $b_{\rm eff} = 2.1$. Our model implies $\log(M_{\rm min}/M_\odot) \simeq 12.4$ for sources with $S_{450\mu{\rm m}} > 5$ mJy and $\log(M_{\rm min}/M_\odot) \simeq 13.0$ for sources with $S_{850\mu{\rm m}} > 5$ mJy. The corresponding values of the clustering radius and of the effective bias factor are $r_0 \simeq 11.2\,h^{-1}$ Mpc, $b_{\rm eff} = 4.3$ at $850\,\mu$m, and $r_0 \simeq 7.3\,h^{-1}$ Mpc, $b_{\rm eff} = 3.1$ at $450\,\mu$m. The study by Kim et al. (2011) confirms that the clustering data require a higher amplitude of the 2-halo term, i.e. more massive halos than implied by the major mergers plus top-heavy initial stellar mass function scenario.

Davé et al. (2010) investigated the clustering properties of rapidly star-forming galaxies at $z \simeq 2$ in the framework of a very different scenario based on cosmological hydrodynamic simulations whereby the star formation is not powered by mergers but by steady gas accretion and cooling that can fuel the star formation for several Gyrs. In this scenario typical sub-mm galaxies at $z = 2$ live in massive ($\sim 10^{13}\,M_\odot$) halos and have a duty cycle $\simeq 50\%$. They are expected to be strongly clustered, with a clustering radius $r_0 \sim 10\,h^{-1}$ Mpc and a bias factor of ~ 6. These values are well in excess of those following from our analysis which yields, for the bulk of galaxies at $z \simeq 2$, $r_0 \simeq 6.9\,h^{-1}$ Mpc, $b_{\rm eff} \simeq 3$.

These results illustrate the power of accurate measurements of the CIB power spectrum and of the correlation function of galaxies at (sub-)millimeter wavelengths to discriminate among competing evolutionary models for the population of dusty galaxies.

ACKNOWLEDGMENTS

Thanks are due to G. Lagache for clarifications on the CIB power spectra derived from *Planck* data and to the referee for a careful reading of the manuscript and useful comments. Our numerical analysis was performed on the Deepcomp 7000 system of the Supercomputing Center of Chinese Academy of Sciences. We acknowledge financial support from ASI (ASI/INAF Agreement I/072/09/0 for the Planck LFI activity of Phase E2) and MIUR PRIN 2009. MV is supported by ASI/AAE, PD-INFN 51, PRIN INAF and the FP7 cosmoIGM grants.

REFERENCES

Addison G. E., et al., 2011, arXiv:1108.4614
Almeida C., Baugh C. M., Lacey C. G., 2011, MNRAS, 417, 2057
Amblard A., et al., 2011, Natur, 470, 510
Baugh C. M., Lacey C. G., Frenk C. S., Granato G. L., Silva L., Bressan A., Benson A. J., Cole S., 2005, MNRAS, 356, 1191
Blain A. W., Chapman S. C., Smail I., Ivison R., 2004, ApJ, 611, 725
Bullock J. S., Kolatt T. S., Sigad Y., Somerville R. S., Kravtsov A. V., Klypin A. A., Primack J. R., Dekel A., 2001, MNRAS, 321, 559
Cooray A., Sheth R., 2002, PhR, 372, 1
Cooray A., et al., 2010, A&A, 518, L22
Cox P., et al., 2011, ApJ, 740, 63
Das S., et al., 2011, ApJ, 729, 62
Davé R., Finlator K., Oppenheimer B. D., Fardal M., Katz N., Kereš D., Weinberg D. H., 2010, MNRAS, 404, 1355
Dekel A., Sari R., Ceverino D., 2009, ApJ, 703, 785
de Zotti G., Ricci R., Mesa D., Silva L., Mazzotta P., Toffolatti L., González-Nuevo J., 2005, A&A, 431, 893
Dunkley J., et al., 2011, ApJ, 739, 52
Eales S., et al., 2010, PASP, 122, 499
Granato G. L., De Zotti G., Silva L., Bressan A., Danese L., 2004, ApJ, 600, 580
Granato G. L., Silva L., Monaco P., Panuzzo P., Salucci P., De Zotti G., Danese L., 2001, MNRAS, 324, 757
Hall N. R., et al., 2010, ApJ, 718, 632
Hawkins E., Maddox S., Branchini E., Saunders W., 2001, MNRAS, 325, 589
Ivison R. J., et al., 2010, A&A, 518, L35
Kennicutt R. C., Jr., 1998, ARA&A, 36, 189
Kim H.-S., Lacey C. G., Cole S., Baugh C. M., Frenk C. S., Efstathiou G., 2011, arXiv, arXiv:1111.0721
Kitayama T., Suto Y., 1996, ApJ, 469, 480
Lacey C. G., Baugh C. M., Frenk C. S., Benson A. J., Orsi A., Silva L., Granato G. L., Bressan A., 2010, MNRAS, 405, 2
Lapi A., Shankar F., Mao J., Granato G. L., Silva L., De Zotti G., Danese L., 2006, ApJ, 650, 42
Lapi A., et al., 2011, ApJ, 742, 24
Lapi A., Cavaliere A., 2011, ApJ, 743, 127
Lewis A., Challinor A., Lasenby A., 2000, PRD, 538, 473
Maddox S. J., et al., 2010, A&A, 518, L11

Mann B., Saunders W., Taylor A., 1995, astro, arXiv:astro-ph/9511028

Mao J., Lapi A., Granato G. L., de Zotti G., Danese L., 2007, ApJ, 667, 655

Millea M., Doré O., Dudley J., Holder G., Knox L., Shaw L., Song Y.-S., Zahn O., 2011, arXiv:1102.5195

Narayanan D., Cox T. J., Hayward C. C., Younger J. D., Hernquist L., 2009, MNRAS, 400, 1919

Narayanan D., et al., 2010, MNRAS, 407, 1701

Navarro J. F., Frenk C. S., White S. D. M., 1996, ApJ, 462, 563

Negrello M., Perrotta F., González-Nuevo J., Silva L., de Zotti G., Granato G. L., Baccigalupi C., Danese L., 2007, MNRAS, 377, 1557

Pénin A., Doré O., Lagache G., Béthermin M., 2011, arXiv:1110.0395

Planck Collaboration, 2011, A&A, 536, A18

Renzini A., 2006, ARA&A, 44, 141

Scott S. E., Dunlop J. S., Serjeant S., 2006, MNRAS, 370, 1057

Shang C., Haiman Z., Knox L., Oh S. P., 2011, arXiv:1109.1522

Sheth R. K., Tormen G., 1999, MNRAS, 308, 119

Shirokoff E., et al., 2011, ApJ, 736, 61

Swinbank A. M., et al., 2010, Natur, 464, 733

Tacconi L. J., et al., 2008, ApJ, 680, 246

Tinker J. L., Wetzel A. R., 2010, ApJ, 719, 88

Viero M. P., et al., 2009, ApJ, 707, 1766

Wang J., et al., 2011, MNRAS, 413, 1373

Weinberg N. N., Kamionkowski M., 2003, MNRAS, 341, 251

Wilman R. J., Röttgering H. J. A., Overzier R. A., Jarvis M. J., 2003, MNRAS, 339, 695

Zhao D. H., Mo H. J., Jing Y. P., Börner G., 2003, MNRAS, 339, 12

Zheng Z., et al., 2005, ApJ, 633, 791